Biosensors and Bioelectronics 49 (2013) 118–125

Contents lists available at SciVerse ScienceDirect

Biosensors and Bioelectronics

journal homepage: www.elsevier.com/locate/bios

A multiplexed microfluidic platform for rapid antibiotic susceptibility testing

Ritika Mohan [1], Arnab Mukherjee [1], Selami E. Sevgen, Chotitath Sanpitakseree, Jaebum Lee, Charles M. Schroeder, Paul J.A. Kenis *

Department of Chemical & Biomolecular Engineering, University of Illinois at Urbana-Champaign, 600 South Mathews Avenue, Urbana, IL 61801, USA

ARTICLE INFO

Article history:
Received 30 March 2013
Accepted 25 April 2013
Available online 9 May 2013

Keywords:
Antibiotic susceptibility testing
Green fluorescent protein (GFP)
Microfluidics
Fluorescence detection
Multiplexed sensor

ABSTRACT

Effective treatment of clinical infections is critically dependent on the ability to rapidly screen patient samples to identify antibiograms of infecting pathogens. Existing methods for antibiotic susceptibility testing suffer from several disadvantages, including long turnaround times, excess sample and reagent consumption, poor detection sensitivity, and limited combinatorial capabilities. Unfortunately, these factors preclude the timely administration of appropriate antibiotics, complicating management of infections and exacerbating the development of antibiotic resistance. Here, we seek to address these issues by developing a microfluidic platform that relies on fluorescence detection of bacteria that express green fluorescent protein for highly sensitive and rapid antibiotic susceptibility testing. This platform possesses several advantages compared to conventional methods: (1) analysis of antibiotic action in two to four hours, (2) enhanced detection sensitivity (≈1 cell), (3) minimal consumption of cell samples and antibiotic reagents ($< 6\ \mu L$), and (4) improved portability through the implementation of normally closed valves. We employed this platform to quantify the effects of four antibiotics (ampicillin, cefalexin, chloramphenicol, tetracycline) and their combinations on *Escherichia coli*. Within four hours, the susceptibility of bacteria to antibiotics can be determined by detecting variations in maxima of local fluorescence intensity over time. As expected, cell density is a major determinant of antibiotic efficacy. Our results also revealed that combinations of three or more antibiotics are not necessarily better for eradicating pathogens compared to pairs of antibiotics. Overall, this microfluidic based biosensor technology has the potential to provide rapid and precise guidance in clinical therapies by identifying the antibiograms of pathogens.

© 2013 Elsevier B.V. All rights reserved.

1. Introduction

In recent years, antibiotic resistance traits among microbial pathogens have escalated at alarming rates, which has spurred the development of technologies for rapid and accurate detection of antibiotic susceptibility profiles of pathogens (Rice, 2010). Established techniques for antibiotic susceptibility testing (AST), such as broth dilution and disc diffusion, involve multiple time-consuming steps (Lazcka et al., 2007; White et al., 1996) including: (1) isolation of pathogens from patient samples (24–48 h.), (2) pre-culturing of isolated bacteria to enrich cell density to detectable levels (24–48 h.), (3) incubation of cells with antibiotics in 96-well plates or petri dishes (24–48 h.), and (4) determination of bacterial growth using absorption spectroscopy or by visual assessment. Broth dilution and disc diffusion assays typically require significant quantities (10–30 mL) of patient samples such as blood, sputum, or urine for analysis (Mancini et al., 2010). In addition, the limited sensitivity of macroscale techniques for AST makes them unsuitable for detecting the presence of "persister" microbes. Although persister cells represent only a small fraction ($\approx 10^{-5}$) of microbial cells, they tend to evade antibiotic mediated killing by switching to a metabolically dormant or "persistent" state (Balaban et al., 2004; Lewis, 2010). Persister cells constitute a significant threat due to their ability to re-initiate infection upon discontinuation of antibiotic therapy (Dawson et al., 2011). Finally, inconsistencies in results obtained from different AST techniques further complicate diagnosis and treatment (Gales et al., 2001; Goldstein et al., 2007; Lo-Ten-Foe et al., 2007; Nicodemo et al., 2004; Tan and Ng, 2007; Traub, 1970). Hence, in the absence of precise information about the antibiogram of particular pathogen, physicians often resort to empirical therapies that utilize broad-spectrum antibiotics. Indiscreet use of antibiotics in this manner is known to intensify the problem of antibiotic resistance (Alanis, 2005; Ang, 2001).

To address the aforementioned issues, biosensor platforms with improved sensitivity and fast analysis time have been developed for

* Corresponding author. Tel.: +1 217 265 0523; fax: +1 217 333 5052.
E-mail address: kenis@illinois.edu (P.J.A. Kenis).
[1] *These authors contributed equally to the work.*

0956-5663/$ - see front matter © 2013 Elsevier B.V. All rights reserved.
http://dx.doi.org/10.1016/j.bios.2013.04.046

antimicrobial susceptibility testing (Chiang et al., 2009; Karasinski et al., 2007; Kinnunen et al., 2011; Koydemir et al., 2011; Nakamura et al., 1991; Tsou et al., 2010). For example, electrochemical sensors have been utilized to determine susceptibility by measuring small changes in growth of cells (Karasinski et al., 2007). Chiang et al., have developed a surface plasmon resonance-based biosensor platform to categorize strains as susceptible or resistant by detecting variations in optical properties of bacteria when treated with antibiotics (Chiang et al., 2009). Another interesting approach for antibiotic susceptibility testing utilizes an asynchronous magnetic bead rotation biosensor to monitor single cells or cell populations after treatment with antibiotics (Kinnunen et al., 2011). In addition, filter chip and optical detection biosensing system have been developed that can provide susceptibility results in one hour (Tsou et al., 2010). These microfluidic-based biosensor technologies are sensitive and rapid, however, most of these platforms lack multiplexing capabilities (Chiang et al., 2009; Kinnunen et al., 2011; Tsou et al., 2010). Hence, integrated microfluidics represents an attractive technology for the multiplexed implementation of biological assays with rapid turnaround times and minimal sample consumption (Sia and Whitesides, 2003). Several successful microfluidic platforms for AST have been reported (Boedicker et al., 2008; Chen et al., 2010; Churski et al., 2012; Cira et al., 2012; Ho et al., 2012; Kalashnikov et al., 2012; Sun et al., 2011). For example, droplet-based microfluidics has been utilized to compartmentalize bacterial cells, nutrients, antibiotics, and fluorescent viability indicators in water-in-oil emulsions (Boedicker et al., 2008; Churski et al., 2012). Sun et al. have reported on the development of a microfluidic platform for the confinement of bacterial cells in square microwells connected to a central flow channel that continuously delivers nutrients and antibiotics to cells (Sun et al., 2011). Choi et al. have reported a microfluidic agarose channel system for rapid antibiotic susceptibility testing by tracking single cell growth (Choi et al., 2013). Weibel and colleagues have developed a portable microfluidic chip for AST for point-of-care use (Cira et al., 2012). The key advantage of the portable chip is the automatic loading of bacterial cells into microfluidic chambers that had been preloaded with dehydrated antibiotics using a 'degas driven flow'.

The existing approaches for microfluidic-based antibiotic susceptibility testing offer promising routes toward the development of a rapid and portable screening tool. However, many of these methods suffer from one or more of the following limitations: (1) complicated platform fabrication and/or operation procedures (Kalashnikov et al., 2012), (2) poor portability due to the requirement for syringe pumps, pneumatic actuators, and other ancillary equipment (Choi et al., 2013; Churski et al., 2012; Kalashnikov et al., 2012), and (3) unstable droplet formation (Theberge et al., 2010). In this work, we report on the design and fabrication of a microfluidic platform with biosensing capabilities featuring a spatially addressable 4×6-array of wells to simultaneously monitor the effects of multiple antibiotics at different concentrations, as well as their combinations, on bacterial cells for AST. This technology integrates ease-of-fabrication and use with enhanced combinatorial capabilities, and further provides improved portability and usability by circumventing the requirement for expensive syringe pumps and pneumatic actuators by implementing normally closed valves. In addition, the platform is amenable to automated analysis by using time-lapse fluorescence microscopy (TLFM). We employed the microfluidic platform to interrogate the antibiotic sensitivity profile of *Escherichia coli* to four commonly used bactericidal and bacteriostatic antibiotics. Furthermore, we explored synergistic and antagonistic effects of different antibiotic cocktails, as well as the effects of *E. coli* cell densities on dictating the efficiency of antibiotic action. Overall, this platform capitalizes on several key advantages of biosensor based integrated microfluidics technology including miniaturization of assays, expedited analysis, multiplexing, and improved detection sensitivity along with ease-of-use and portability.

2. Materials and Methods

2.1. Microfluidic chip fabrication

The microfluidic chip for AST was fabricated using standard soft lithographic techniques (Xia and Whitesides, 1998). Briefly, molds for casting the fluidic and control layers were made by patterning negative photoresist on silicon wafers using photolithography. A thin layer of 20:1 PDMS (weight ratio of polymer to cross-linker) was spin coated on to the fluidic layer master and 5:1 PDMS was poured on to the control layer master. The two layers were partially cured at 65 °C for 30 minutes. Next, the control layer was carefully peeled off the silanized silicon master, and three holes for actuation of the mixing and sample loading valves were punched using a 20-gauge needle. The control layer was manually aligned with the fluidic layer under an optical microscope (Leica MZ6), and the aligned layers were cured overnight (~12 h.) at 65 °C to yield a monolithic device. Finally, the assembled device was peeled off the fluid layer master, inlet ports were punched using a 20-gauge needle, and the assembly was placed on a glass coverslip to create a reversible seal.

2.2. Bacterial strains, growth media, and antibiotic solutions

Wild type *Escherichia coli* MG1655 (ATCC 47076) was genetically engineered to constitutively express green fluorescent protein (GFP), thereby enabling detection and enumeration of cells using fluorescence microscopy. Specifically, *E. coli* MG1655 cells were transformed with a low copy plasmid expressing a bright GFP variant from a constitutive promoter derived from bacteriophage lambda (Lutz and Bujard, 1997). Details of plasmid construction are provided as supporting information (Table A.1). We verified that the recombinant GFP-expressing *E. coli* cells were phenotypically similar to wild type cells with respect to growth rates. *E. coli* cells were routinely cultivated in Lennox broth (10 g/L tryptone, 5 g/L yeast extract, and 5 g/L NaCl) supplemented with kanamycin at a concentration of 30 μg/mL in order to maintain the GFP-expressing plasmid. Kanamycin was omitted for on-chip cultures with no noticeable effect on cellular fluorescence. Antibiotic stock solutions of 10 mg/mL tetracycline hydrochloride and 10 mg/mL chloramphenicol were prepared in 70% ethanol. Stock solutions of 30 mg/mL kanamycin, 100 mg/mL ampicillin, and 1 mg/mL cefalexin hydrate were prepared in sterile deionized water. All stock solutions were filtered using a 0.45 μm syringe filter (Millex- HV filter unit, Millipore) prior to use. Antibiotic dilutions were made directly into Lennox broth. The antibiotics tetracycline, chloramphenicol, and cefalexin hydrate were purchased from Sigma-Aldrich, and kanamycin and ampicillin were purchased from Fisher Scientific.

2.3. On-chip antibiotic susceptibility testing

Microfluidic chips were sterilized by autoclaving prior to each experiment. Nonspecific interactions between the chip surface and cells or antibiotics were minimized by passivating the walls of the fluid layer and the glass coverslip with sterile bovine serum albumin (BSA) at a concentration of 10 mg/mL for 15 min before each experiment. In a typical experiment (Fig. A.1), the microfluidic chip-cover slip assembly is placed in contact with an aluminum-heating block heated to 35 °C using a temperature controller (Bionomic System BC-110). Antibiotic and cell solutions (≈1 μL volume for each) are placed on their respective inlet ports and introduced into the wells by actuating the filling valves using a vacuum pump

(3 psig; GastDOA-P704-AA VacuumPump 1/8 HP 115 VAC). Enhanced mixing of adjacent sets of antibiotic and cell solutions is initiated by actuating the mixing valves for 15 min. To minimize solvent loss due to evaporation during long-term experiments, reservoirs filled with bacterial growth medium (Lennox broth) or sterile water were placed around the device, and the assembly was sealed at the top by affixing a glass slide (Fig. A.1). On-chip measurements were performed by TLFM using an inverted fluorescence microscope (Leica, DMI4000) equipped with a 1600 × 1200 pixel CCD camera (QImaging, Retiga-2000R), a 480/40 nm excitation filter, 527/30 nm emission filter, a motorized stage to raster the imaging field-of-view, and automated focus control implemented with a Z-motor (Ludl Electronic Products). Images were acquired every 10 min over a period of 10 h using a 10x objective (Plan Achromat, $NA=0.25$). The shallow fluid channels (15 μm) ensured that all cells were within the depth of focus throughout the experiment. During data acquisition, the exposure time was set to 200 ms and the fluorescent light source was shuttered between successive exposures to minimize photobleaching. Stage rastering, focus control, image acquisition, and capture were implemented using ImagePro Plus software (Media Cybernetics).

2.4. Image processing and data analysis

Images were analyzed using ImageJ version 1.46a (Rasband, 2011). Specifically, 8-bit grayscale images were converted to binary images by manual thresholding to capture all cells within a range of fluorescence intensities, which is defined on the low end by a minimum signal-to-noise ratio and determined on the high end by the inability to visualize cells. The number of cells in each chamber was also estimated by counting the local fluorescence intensity maxima, and this algorithm provided consistent results within this range of manual thresholding. In order to highlight long-term trends in cell proliferation (or death), we implemented a moving average filter to smooth the time series data. We quantified antibiotic efficacy in terms of the fraction of the initial cell population that survives antibiotic treatment after 10 h, which is estimated as

$$FL_{ab,conc} = \frac{N_{10}}{N_0} \tag{1}$$

where $FL_{ab,conc}$ denotes the fraction of live cells at $t=10$ h., subscripts *ab* and *conc* refer to the antibiotic and its concentration in units of μg/mL, N_o is the total number of cells in a microfluidic chamber at $t=0$, and N_{10} is the total number of cells in the same chamber at $t=10$ h. Synergy and antagonism between pairs of antibiotics are calculated using a criterion variable A:

$$A = \frac{FL_{ab1+ab2}}{min(FL_{ab1},\ FL_{ab2})} \tag{2}$$

where $FL_{ab1+ab2}$ denotes the fraction of live cells at $t=10$ h post-treatment with a pair of antibiotics ($ab1+ab2$), and FL_{ab1} and FL_{ab2} denote the fraction of live cells at $t=10$ h post-treatment with each antibiotic individually at the same concentration as in the combination (in a different experiment). Using this convention, an antibiotic combination is defined as being synergistic if $A<1$ and antagonistic if $A>1$. For experiments involving combinations of three or four antibiotics, this definition of A was extended to account for combinatorial treatment methods (Eqs (A.(1) and A.2) in Appendix A).

2.5. Antibiotic susceptibility testing in 96-well format (macroscale)

To benchmark our microfluidic platform against macroscale methods for antibiotic screening, we performed antibiotic susceptibility testing on *E. coli* using 96-well plates. *E. coli* cell cultures were prepared as described above and added to the wells of a 127.8 mm × 85.5 mm flat-bottom 96-well plate (Nunclon). Antibiotics were added to each well at the desired concentrations, and the plates were incubated at 35 °C with linear shaking (linear mode, 3.5 mm amplitude) in a microplate reader (TECAN Infinite M200 PRO). Cell growth or death was monitored by recording optical density at a wavelength of 600 nm in each well every 15 min over a period of 15 h. In bulk-level experiments, evaporation was minimized by using covered plates.

3. Results and discussion

3.1. Design and validation of the microfluidic platform for biological studies

The microfluidic platform used in this study (Fig. 1) consists of a two-layer poly (dimethyl-siloxane) chip comprising: (1) a control layer for actuating the mixing and filling valves, and (2) a fluidic layer that houses the flow channels and a 4 × 6-array of wells. Each well consists of two half wells that house the cells and antibiotic solutions, respectively. Each half well is 400 μm wide, 15 μm tall and 500 μm long. In this way, the 4 × 6 array design facilitates the treatment of one microbial cell sample with six distinct antibiotic solutions,

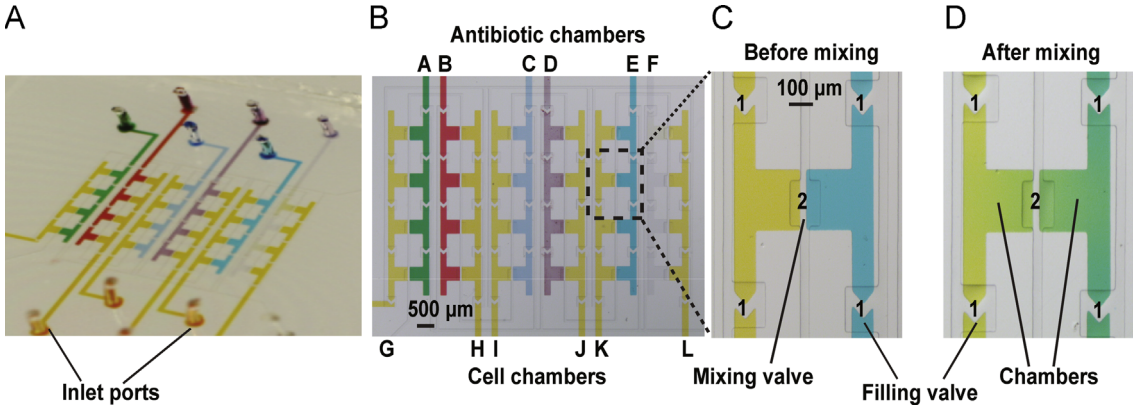

Fig. 1. Optical micrographs of the microfluidic platform for on-chip AST: **(A)** The device features a 4 × 6 array of 3 nL volume wells, which are loaded with colored dyes for display purposes. **(B)** Antibiotics at various concentrations and/or different antibiotic combinations are loaded in each well through fluid lines A–F (represented by green, red, blue, magenta, indigo and colorless solutions). *E. coli* cells are loaded in the wells adjacent to the antibiotics through fluid lines G-L (represented by yellow solutions). **(C)** Normally-closed pneumatic valve set 1 is used to control the antibiotic and cell loading in the wells. **(D)** Actuation of mixing valve set 2 is used to mix the antibiotics and cells in adjacent chambers by enhanced diffusion, represented by a change in colors (blue/yellow to green) in the optical micrographs. (For interpretation of the references to color in this figure legend, the reader is referred to the web version of this article.)

thereby enabling the execution of up to six unique screens per chip along with four replicates for each screen (Fig. 1). Antibiotic solutions and cell samples are readily loaded and mixed by actuating the respective filling and mixing valves using a vacuum pump. The incorporation of normally closed valves improves platform portability by obviating the need for continuous actuation using positive pressure (Mohan et al., 2011; Schudel et al., 2009; Schudel et al., 2011; Thorson et al., 2011). To validate the feasibility of the microfluidic platform for biological studies, we determined the doubling times of *E. coli* cultured on-chip and in 96-well plates using two different kinds of media: nutrient-rich Lennox medium and minimal glucose-based M9 medium. We verified that the on-chip growth profiles of *E. coli* cells were in close agreement with the growth profiles observed in the 96-well plate based experiments (Fig. A.2). Specifically, the on-chip doubling times of *E. coli* were approximately 35 min and 70 min in Lennox broth and M9 medium, respectively. The corresponding doubling times in the same media when using 96-well plates were 30 min and 73 min, respectively. The general scheme of the sensing system is shown in Fig. A.3.

3.2. Effects of individual antibiotics on E. coli cells

We employed the microfluidic screening chip to investigate the effects of four widely prescribed antibiotics on *E. coli* expressing GFP. The use of GFP as a genetically encodable indicator of cell viability has been previously reported (Keymer et al., 2006). Transformation of bacteria to express GFP is a standard procedure routinely used in microbiology or for applications in monitoring cell growth over an extended period of time. Antibiotics were selected to comprise bactericidal (ampicillin, cefalexin) and bacteriostatic (tetracycline, chloramphenicol) classes. We treated early log-phase cultures of *E. coli* with varying concentrations of each antibiotic on-chip and quantified cell numbers using TLFM over a period of 10 h (Fig. 2). Representative optical images showing action of an antibiotic on bacteria over a period of 10 h are shown in Fig. A.4. Although cell numbers are quantified over a period of 10 h, antibiotic susceptibility information is discernible within 2–4 h (Fig. A.5). We estimated antibiotic efficiency in terms of the fraction of the initial cell population in a chamber that survives antibiotic treatment at the end of an experiment ($FL_{ab,\ conc}$) as defined by Eq. (1). $FL_{ab,\ conc}$ values are tabulated in Table 1. In case of unperturbed cell growth (no antibiotics added), *FL* typically has a value close to 166, which corresponds to 6–8 population doubling events over a period of 10 h. Bactericidal (cell killing) antibiotic action is expected to result in a value of $FL_{ab,conc} < 1$, whereas bacteriostatic (growth arresting) antibiotic action will lead to $FL_{ab,conc} \approx 1$. In this way, $FL_{ab,conc}$ serves as a robust measure of antibiotic potency.

We observed that all four antibiotics failed to inhibit cell growth when employed at low concentrations (0.5 μg/mL), although the final cell densities (at $t = 10$ h.) are considerably lower than in the case where cells are not treated with antibiotics ($FL_{amp,0.5} \approx 15.4$, $FL_{cef,0.5} \approx 23.5$, $FL_{chl,0.5} \approx 29.2$, and $FL_{tet,0.5} \approx 32.9$). At a 10-fold higher concentration (5 μg/mL), ampicillin results in a substantial amount of cell death by lysis ($FL_{amp,5} \approx 0.55$), whereas tetracycline and chloramphenicol almost completely abrogate cell division without causing significant lysis ($FL_{tet,5} \approx 1.21$, *and* $FL_{chl,5} \approx 1.24$). These results are consistent with the bactericidal

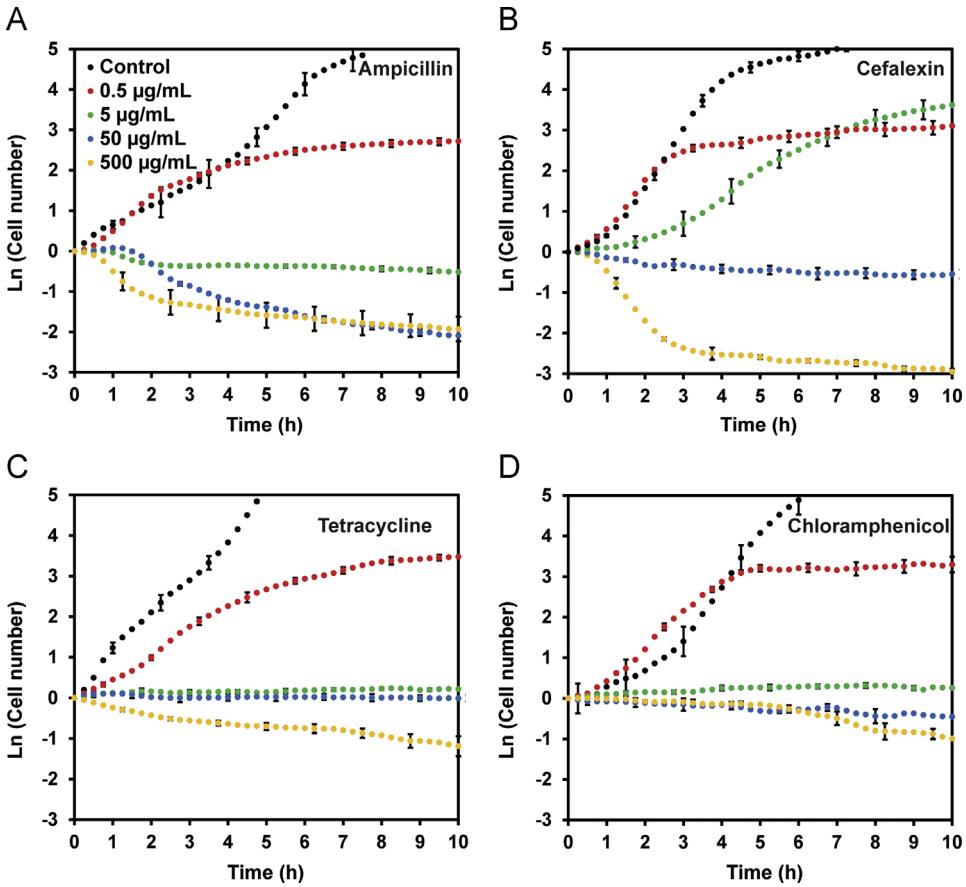

Fig. 2. Effects of individual antibiotics on *E. coli* growth using an on-chip assay. Time traces represent the effects of bactericidal antibiotics: **(A)** ampicillin and **(B)** cefalexin and bacteriostatic antibiotics: **(C)** tetracycline and **(D)** chloramphenicol on cell growth. Cell growth and death were monitored by counting cells in each well, every 10 min, over a period of 10 hours. Cell numbers are normalized to the initial ($t = 0$) value. Each data point represents the mean of measurements from three experiments. Error bars represent the standard error of the mean (SEM) and are depicted for every fifth data point for visual clarity.

and bacteriostatic mode of action of the respective antibiotics. Interestingly, cell proliferation is observed in the case of cefalexin ($FL_{cef,5}$≈33.2). At the highest concentration (500 μg/mL), we observed significant cell death for all antibiotics ($FL_{amp,500}$≈0.16 and $FL_{cef,500}$≈0.06; $FL_{tet,500}$≈0.33 and $FL_{chl,500}$≈0.37).

Cell growth data obtained using the on-chip microfluidic assay are generally in good agreement with those obtained in the 96-well plate assays, albeit with a few notable differences (Fig. A.6). In particular, 96-well plate based assays revealed robust cell growth upon treatment with cefalexin at 50 μg/mL, whereas complete growth arrest was observed using the on-chip assay for the same antibiotic concentration ($FL_{cef,50}$≈0.58). This difference can be explained by the different ways in which cell density is determined using the microfluidic on-chip assay versus the bulk-level 96-well plate assay. At a concentration of 50 μg/mL, cefalexin causes massive cell filamentation because it inhibits cell wall synthesis in *E. coli*. Indeed, in on-chip experiments, we observed a nearly 20-fold increase in cell length within 4 h of cefalexin treatment (Fig. A.7). Cell elongation contributes to increased absorbance at 600 nm; however, in bulk assays that rely on optical absorbance to quantify cell growth, cell filamentation is perceived as an increase in cell density. In an analogous fashion, in the early stages (t≈1.5 h.) of ampicillin treatment (5 μg/mL) and cefalexin treatment (50 and 500 μg/mL), cell filamentation is misconstrued as rapid growth by the bulk absorbance based assay performed in the 96-well plates (See Figs. A.7 and A.8). In this way, the microfluidic-based assay relies on single cell measurements to determine the efficacy of treatment, which intrinsically results in a more accurate measure of antibiotic potency.

A second important difference between bulk-level AST and microfluidic-based AST is the possibility of antibiotic precipitation at high concentrations, which can obscure absorbance measurements in bulk-level analysis. We observed this phenomenon in the case of tetracycline. Based on 96-well plate measurements, the highest concentration of tetracycline (500 μg/mL) fails to inhibit cell growth initially (up to t≈1.5 h.), whereas the same concentration results in cell lysis using the on-chip assay ($FL_{tet,500}$≈0.33). Moreover, inhibition of cell growth by tetracycline appears to be more effective at lower concentrations of the antibiotic (5 and 50 μg/mL). We attribute this discrepancy to the rapid precipitation of tetracycline in aqueous solution at concentrations exceeding 500 μg/mL (Martindale, 1989). Precipitation of tetracycline from solution in the bulk-level assays results in an erroneous ~3-fold increase in optical absorbance at 600 nm ($Abs_{600,\ 0.5\ mg/L\ tet}$=0.25 versus $Abs_{600,\ blank}$=0.08). In addition, it is well known that hydrophobic small molecules can be absorbed by PDMS. Therefore, we performed a series of control experiments to ensure that the on-chip antibiotic concentrations in our microfluidic platform were not significantly perturbed during the course of our experiments (Table A.2). We quantified antibiotic concentrations before and after on-chip incubation for 10 h using liquid chromatography-mass spectrometry (LC-MS). Based on mass spectrometry, ampicillin, cefalexin, and chloramphenicol showed no significant absorption by PDMS. However, we observed some degree of absorption in case of tetracycline at the endpoint of prolonged 10-hour incubation in PDMS devices. Nevertheless, the on-chip AST results followed the same general trends compared to bulk-level growth experiments, including growth inhibition at low concentrations of tetracycline (5 μg/mL), which is consistent with 96-well plate measurements (Fig. 2).

Table 1
Efficacy of individual antibiotics quantified in terms of *FL* values.

Conc (μg/mL)	FL_{amp}	FL_{cef}	FL_{chl}	FL_{tet}
500	0.16 ± 0.05	0.06 ± 0.00	0.37 ± 0.01	0.33 ± 0.01
50	0.12 ± 0.01	0.58 ± 0.06	0.66 ± 0.02	1.00 ± 0.08
5	0.55 ± 0.04	33.16 ± 3.82	1.24 ± 0.08	1.21 ± 0.04
0.5	15.44 ± 1.41	23.45 ± 3.93	29.19 ± 5.99	32.86 ± 2.57

3.3. Effects of antibiotics tested in pairs

The development of novel antimicrobials has lagged in pace relative to the rapid emergence of microbial drug resistance against several existing antibiotics (Keith et al., 2005). In the absence of new potent pharmaceuticals, multidrug resistant pathogens are frequently treated with combinations of two or more antibiotics. Combination therapy offers a potential way to mitigate the emergence of drug resistance traits because microbial pathogens are less likely to simultaneously develop mutations that render them resistant to multiple antibiotics (Chait et al., 2007; Mouton, 1999). However, interactions between multiple antibiotics may exhibit either synergistic or antagonistic behavior, wherein the combination shows improved or decreased efficiency compared to each antibiotic applied individually. To evaluate the effects of antibiotic combinations on *E. coli* cell growth, we treated cells with the aforementioned antibiotics administered in pairs at a concentration of 5 μg/mL per antibiotic (Fig. 3). In this way, we selected an antibiotic concentration that is lower than the antibiotic minimal inhibitory concentration (MIC) that we determined

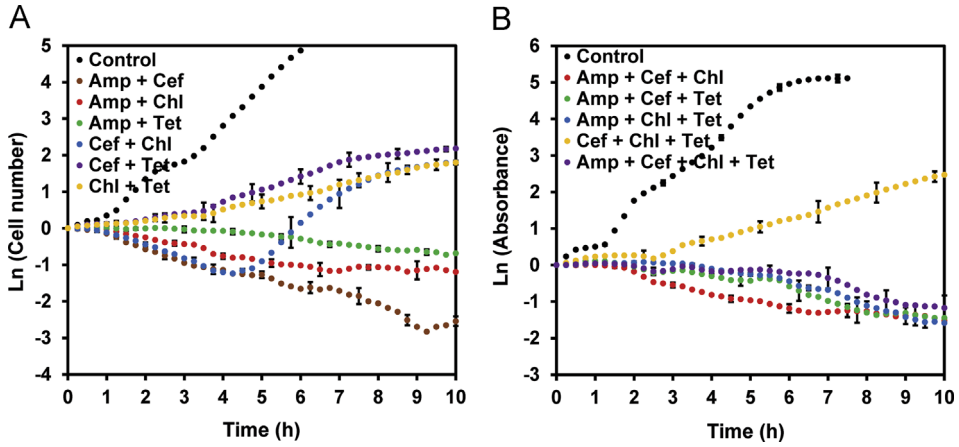

Fig. 3. Synergistic and antagonistic effects of antibiotic combinations on *E. coli*. Time traces represent the effects of **(A)** pairs of antibiotics and **(B)** combinations of 3 and 4 antibiotics on *E. coli* cell growth. All values are normalized to the initial (t=0) cell number. Each data point represents the mean of at least three experiments. Errors bars represent the standard error of the mean (SEM) and are depicted for every fifth data point for visual clarity.

using 96-well plates (Table A.3). Discernible changes in cell numbers were obtained within 4 h of antibiotic treatment (Fig. A.9). We quantify synergistic or antagonistic behavior of a pair of antibiotics based on its ability to eradicate bacterial cells relative to the action of each antibiotic applied individually. For each antibiotic pair, we calculate the value of a criterion variable A as defined above in Eq. (2). Synergistic combinations of antibiotics successfully eradicate *E. coli* cells more effectively than any individual antibiotic ($A < 1$). In contrast, a combination is deemed antagonistic if it eliminates fewer cells relative to the most potent single antibiotic used in the combination ($A > 1$).

Table 2 lists the FL and A values that we determined for each antibiotic pair after performing the corresponding on-chip experiment. This data indicates that the ampicillin-cefalexin pair exhibited the best antibacterial activity ($FL_{amp+cef} \approx 0.06$). In contrast, neither ampicillin nor cefalexin exhibit appreciable cell killing activity when used individually at 5 μg/mL. Our results indicate that a high degree of synergy occurs when the two antibiotics are used in combination ($A = 0.11$). Indeed, synergism between beta-lactam antibiotics, like ampicillin and cefalexin, constitutes the clinical basis for their widespread paired application in treating recalcitrant infections (Allewelt et al., 2004; Dejace and Klastersky, 1986).

In contrast, combinations of the bacteriostatic antibiotics, the chloramphenicol-tetracycline pair resulted in antagonistic behavior. Slow cell growth was observed in this case ($FL_{tet+chl} \approx 7.9$, $FL_{tet,5} \approx 1.21$ and $FL_{chl,5} \approx 1.24$). Tetracycline and chloramphenicol exert their bacteriostatic effects by inhibiting protein synthesis through their interactions with the bacterial ribosome. As both antibiotics aim for very similar target sites in the ribosome, antagonism may result from mutual exclusion of the antibiotics from their preferred target sites in cells (Lorian, 1986).

Paired combinations of ampicillin with tetracycline or chloramphenicol proved to be moderately synergistic ($FL_{amp+tet} \approx 0.46$, $FL_{amp+chl} \approx 0.31$) (Cottarel and Wierzbowski, 2007). However, cephalexin resulted in significant antagonism with regards to cell proliferation when combined with tetracycline or chloramphenicol and observed up to 10 h ($FL_{cef+chl} \approx 6.34$, $FL_{cef+tet} \approx 8.85$). Antagonism of growth inhibitory effects of the bacteriostatic antibiotics by cefalexin can be attributed to cefalexin's activity on the bacterial cell wall. Consistent with the mode of action of cephalosporin antibiotics, cefalexin interferes with cell wall peptidoglycan synthesis and compromises the integrity of the bacterial cell wall (Rolinson, 1980). Enhanced cell wall permeability may hinder intracellular retention of chloramphenicol and tetracycline to concentrations sufficient for antibacterial activity (Lorian, 1986). Although ampicillin exerts an analogous effect on the bacterial cell wall, antagonism is likely to be less apparent due to the greater potency of ampicillin relative to cefalexin (Table A.3). Specifically, as mentioned above, 5 μg/mL ampicillin is sufficient to prevent cell growth, whereas higher concentrations of cefalexin need to be used to accomplish the same effect. Interestingly, *E. coli* cells respond to the cefalexin-chloramphenicol pair in a biphasic manner; herein, an initial phase of cell elongation and rapid lysis (up to $t = 5$ h.) is followed by a period of steady growth. Finally, the microfluidic-based on-chip results agree well with those obtained from 96-well plate assays with similar differences as described in the previous section (Fig. A.10). In particular, cell elongation in the case of antibiotic pairs involving ampicillin or cefalexin is misconstrued as rapid initial growth by the absorbance-based bulk assay.

Table 2
Synergistic/antagonistic interactions of antibiotic combinations.

Combinations	*FL*	*A*	Interaction
Amp+Cef	0.06 ± 0.01	0.11	synergistic
Amp+Chl	0.31 ± 0.04	0.52	synergistic
Amp+Tet	0.46 ± 0.03	0.77	synergistic
Cef+Chl	6.34 ± 0.41	5.12	antagonistic
Cef+Tet	8.85 ± 0.44	7.29	antagonistic
Chl+Tet	7.94 ± 0.45	6.54	antagonistic
Amp+Cef+Chl	0.24 ± 0.04	3.44	antagonistic
Amp+Cef+Tet	0.29 ± 0.12	4.17	antagonistic
Amp+Chl+Tet	0.22 ± 0.01	0.70	synergistic
Cef+Chl+Tet	10.0 ± 2.63	8.23	antagonistic
Amp+Cef+Chl+Tet	0.38 ± 0.16	5.61	antagonistic

3.4. Effect of antibiotics tested in combinations of three and four

Moving beyond simple pairs of antibiotics, we also tested combinations of three and four antibiotics together to assess whether higher order antibiotic combinations could significantly enhance the antibacterial activity compared to antibiotic pairs (Fig. 3). Synergistic or antagonistic interactions between combinations of three or four antibiotics are defined based on the ability of the combination to inhibit cell proliferation relative to the effect of each antibiotic in isolation, as well as to that of sub-groups of antibiotics (pairs and triplets) included in the higher order combination. We calculated the criterion variable A using Eq. (3) in a manner analogous to antibiotic pairs (Table 2). Interestingly, all tested combinations of three or four antibiotics performed worse than the ampicillin-cefalexin pair ($FL_{amp+cef+chl} \approx 0.24$, $FL_{amp+cef+tet} \approx 0.29$, $FL_{amp+chl+tet} \approx 0.22$, $FL_{cef+chl+tet} \approx 10$, $FL_{amp+cef+chl+tet} \approx 0.38$). This key observation suggests that a high degree of antagonism results when combinations of beta lactam antibiotics (ampicillin, cefalexin) are supplemented with one or more bacteriostatic antibiotics (chloramphenicol, tetracycline), with the exception of ampicillin–chloramphenicol–tetracycline, which was the only higher order combination that exhibits synergistic effects ($A = 0.70$). Beta lactam antibiotics rely on active cell division with concomitant synthesis of the bacterial cell wall to exert their effects (Tipper, 1985). Bacteriostatic antibiotics have been known to antagonize the effects of beta lactam antibiotics through their inhibition of protein synthesis and consequent stalling of cell wall synthesis (Winslow et al., 1983). Consistent with our earlier observations, combinations of cefalexin, chloramphenicol, and tetracycline proved to be highly antagonistic ($FL_{cef+chl+tet} \approx 10.0$). Finally, most of the combinations of three and four antibiotics caused substantial cell elongation, which was anomalously interpreted as cell growth by 96-well plate assays (Fig. A.10).

3.5. Effect of cell density on the killing efficacy of antibiotics

The efficiency of an antibiotic in eradicating pathogen populations is critically dependent on the density of the infecting cells (pathogen load) at the site of infection (Udekwu et al., 2009). Dense bacterial populations often successfully counter antibacterial activities of several potent antibiotics through the initiation of complex genotypic responses based on quorum sensing (Butler et al., 2010; Dorr et al., 2009). Bacterial cells colonizing infection sites can rapidly reach very high densities, because these cells are confined in the constrained space of the host organism. In our work, the microfluidic chambers (dimensions 500 μm × 400 μm × 15 μm and

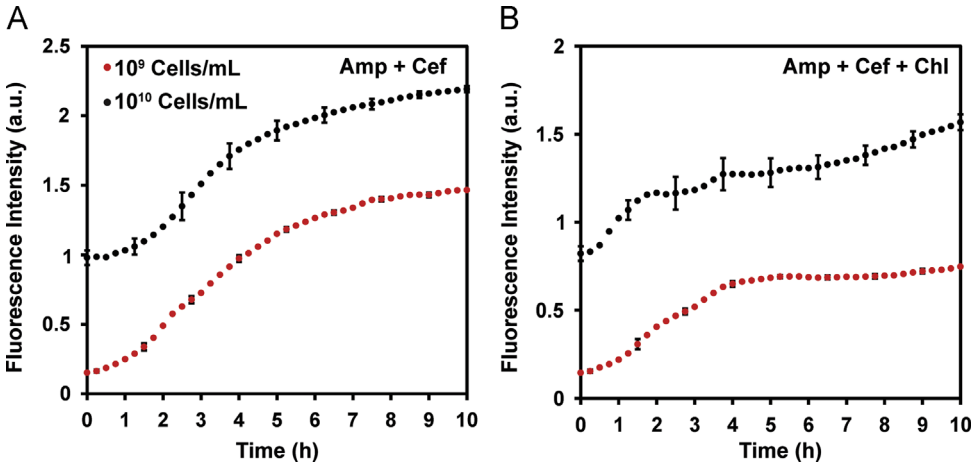

Fig. 4. Effects of initial *E. coli* cell density on antibiotic efficacy. Population effects of *E. coli* cells were investigated for **(A)** a combination of ampicillin and cefalexin and **(B)** combination of ampicillin, cefalexin, and chloramphenicol. Cell growth was quantified by calculating the integrated fluorescence intensity in a microchamber as the dense crowding hindered counting of single cells. Errors bars represent the standard error of the mean (SEM) and are depicted for every fifth data point for visual clarity.

volume = 3 nL) provide a suitable mimic for the microconfinement effects experienced by colonizing pathogens in vivo (Sung and Shuler, 2012). Therefore, we assessed the effects of initial cell density on the killing efficacy of otherwise lethal doses of antibiotics. For this purpose, we chose the most potent antibiotic combination: the ampicillin-cefalexin pair ($FL_{amp+cef} \approx 0.06$ at an initial pathogen load of 10^8 cells/mL). We varied cell densities over two orders of magnitude (10^9–10^{10} cells/mL). Use of high cell densities precludes direct enumeration of cell numbers due to spatial crowding. In these cases, cell growth was quantified by measuring the integrated fluorescence intensity over time in each microchamber. As depicted in Fig. 4, the ampicillin-cefalexin combination proved to be ineffective at cell concentrations of 10^9 cells/mL and 10^{10} cells/mL. We obtained similar results using another potent antibiotic cocktail comprising ampicillin, cefalexin, and chloramphenicol ($FL_{amp+cef+chl} \approx 0.23$). The rapid loss of antibiotic efficiency with 10–100 fold variations in population levels emphasizes the acute need to rapidly establish antibiograms of pathogens before infecting populations escalate to untreatable levels. This further highlights the utility of the microfluidic approach used here, which provides practical information within 4 h. In contract, alternative methods based on current technologies require much longer time (at least 8 h, more typically 24–72 h (Jorgensen and Ferraro, 2009) to provide the same observation.

4. Conclusions

In summary, we have developed a multiplexed microfluidic platform comprised of arrays of small volume chambers (3 nL) that enables monitoring the effects of several antibiotics and their combinations on *E. coli* cells. Conventional methods for antibiotic susceptibility testing (*e.g.*, broth dilution and disc diffusion) are time consuming and tedious, generally requiring large sample and reagent volumes. From this perspective, our microfluidic biosensing platform provides substantial improvements over existing methods with regard to timescale of analysis and sample volumes. In particular, the platform possesses key several advantages such as low sample and reagent volume requirements ($< 6\ \mu L$), enhanced detection sensitivity (~1 cell), rapid turnaround times (2–4 h), improved portability, and enhanced combinatorial capabilities compared to several alternative microfluidic techniques. Even though we quantified antibacterial effects on cells over a total time period of 10 h, changes in cell numbers are already discernible within 2 to 4 h. In this way, the platform substantially accelerates antibiotic susceptibility testing compared to broth dilution and disk diffusion by circumventing the need for pre-culturing cells to detectable levels, which often takes > 24 h. Moreover, our method further enables direct observation and enumeration of cellular phenotypes (growth, morphology). As such, the microfluidic method reported here provides precise quantification of cell numbers, in contrast to bulk methods that rely on population averaged metrics (*e.g.*, optical absorbance) as an indirect proxy for cell number. In addition, the use of normally closed valves in the platform facilitates portability and easy loading of samples and reagents.

On-chip experiments involving combinations of different antibiotics highlight the importance of thorough evaluation of the effectiveness of each combination before use in the clinic. In several instances, antibiotic combinations perform poorly. These results also showcase the utility of the platform for studies like these, as well as for rapid diagnosis and management of infections. The microfluidic platform described in this work relies on genetically modified bacteria for analysis; however, this issue can be circumvented by utilizing fluorescence based or optical dyes. In addition, the methodology reported here relies on the use of fluorescent microscopy, a nearly ubiquitous method that is routinely utilized in medical fields including microbiology, immunology, and pathology testing labs. One can envision using AST chips such as those reported here for further development of point-of-care diagnostic platforms for bacterial infections. To this end, we are currently extending the technology to determine antibiograms of drug resistant microbial pathogens such as *Pseudomonas aeruginosa* and polymicrobial communities.

Moving beyond our current work, the ability of the microfluidic platform to integrate with automated TLFM and to support cell cultures over extended periods of time (up to at least 24 h) makes it a versatile tool for time resolved imaging of live cells in a multiplexed fashion for other applications, including those in the rapidly developing area of systems biology.

Acknowledgments

We acknowledge financial support from the National Science Foundation under awards CMMI 03–28162 and CMMI 07–49028 to Nano-CEMMS; Nano Science & Engineering Center (NSEC) on Nanomanufacturing for PJAK and a Packard Fellowship from the David and Lucile Packard Foundation for CMS. AM was supported

in part by FMC Technologies Graduate Fellowship. We thank Dr. Amit Desai and Dr. Ashtamurthy Pawate for helpful discussions and for proof-reading the manuscript. In addition, we acknowledge Dr. Desai's assistance in designing the antibiotic absorption studies. Finally, we thank Kevin B. Weyant for assistance with bacterial cell cloning.

Appendix A. Supporting information

Supplementary data associated with this article can be found in the online version at http://dx.doi.org/10.1016/j.bios.2013.04.046.

References

Alanis, A.J., 2005. Archives of Medical Research 36 (6), 697–705.
Allewelt, M., Schuler, P., Bolcskei, P.L., Mauch, H., Lode, H., Dalhoff, K., Loos, U., Vogel, F., Wendel, H., von Eiff, C., 2004. Clinical Microbiology and Infection 10 (2), 163–170.
Ang, B.S.P., 2001. Annals of the Academy of Medicine Singapore 30 (2), 199–202.
Balaban, N.Q., Merrin, J., Chait, R., Kowalik, L., Leibler, S., 2004. Science 305 (5690), 1622–1625.
Boedicker, J.Q., Li, L., Kline, T.R., Ismagilov, R.F., 2008. Lab on a Chip 8 (8), 1265–1272.
Butler, M.T., Wang, Q., Harshey, R.M., 2010. Proceedings of the National Academy of Sciences of the United States of America 107 (8), 3776–3781.
Chait, R., Craney, A., Kishony, R., 2007. Nature 446 (7136), 668–671.
Chen, C.H., Lu, Y., Sin, M.L.Y., Mach, K.E., Zhang, D.D., Gau, V., Liao, J.C., Wong, P.K., 2010. Analytical Chemistry 82 (3), 1012–1019.
Chiang, Y.-L., Lin, C.-H., Yen, M.-Y., Su, Y.-D., Chen, S.-J., Chen, H.-f., 2009. Biosensors and Bioelectronics 24 (7), 1905–1910.
Choi, J., Jung, Y.-G., Kim, J., Kim, S., Jung, Y., Na, H., Kwon, S., 2013. Lab on a Chip 13 (2), 280–287.
Churski, K., Kaminski, T.S., Jakiela, S., Kamysz, W., Baranska-Rybak, W., Weibel, D.B., Garstecki, P., 2012. Lab on a Chip 12 (9), 1629–1637.
Cira, N.J., Ho, J.Y., Dueck, M.E., Weibel, D.B., 2012. Lab on a Chip 12 (6), 1052–1059.
Cottarel, G., Wierzbowski, J., 2007. Trends in Biotechnology 25 (12), 547–555.
Dawson, C.C., Intapa, C., Jabra-Rizk, M.A., 2011. PLoS Pathogens 7 (7).
Dejace, P., Klastersky, J., 1986. American Journal of Medicine 80 (6 B), 29–38.
Dorr, T., Lewis, K., Vulic, M., 2009. PLoS Genetics 5 (12).
Gales, A.C., Reis, A.O., Jones, R.N., 2001. Journal of Clinical Microbiology 39 (1), 183–190.
Goldstein, F.W., Ly, A., Kitzis, M.D., 2007. Journal of Antimicrobial Chemotherapy 59 (5), 1039–1040.
Ho, J.Y., Cira, N.J., Crooks, J.A., Baeza, J., Weibel, D.B., 2012. PLoS ONE 7 (7).
Jorgensen, J.H., Ferraro, M.J., 2009. Clinical Infectious Diseases 49 (11), 1749–1755.
Kalashnikov, M., Lee, J.C., Campbell, J., Sharon, A., Sauer-Budge, A.F., 2012. Lab on a Chip.
Karasinski, J., White, L., Zhang, Y., Wang, E., Andreescu, S., Sadik, O.A., Lavine, B.K., Vora, M., 2007. Biosensors and Bioelectronics 22 (11), 2643–2649.
Keith, C.T., Borisy, A.A., Stockwell, B.R., 2005. Nature Reviews Drug Discovery 4 (1), 71–78.
Keymer, J.E., Galajda, P., Muldoon, C., Park, S., Austin, R.H., 2006. Proceedings of the National Academy of Sciences of the United States of America 103 (46), 17290–17295.
Kinnunen, P., Sinn, I., McNaughton, B.H., Newton, D.W., Burns, M.A., Kopelman, R., 2011. Biosensors and Bioelectronics 26 (5), 2751–2755.
Koydemir, H.C., Kulah, H., Ozgen, C., Alp, A., Hascelik, G., 2011. Biosensors and Bioelectronics 29 (1), 1–12.
Lazcka, O., Campo, F.J.D., Munoz, F.X., 2007. Biosensors and Bioelectronics 22 (7), 1205–1217.
Lewis, K., 2010. Persister cells. Annual Review of Microbiology. 64, 357–372.
Lo-Ten-Foe, J.R., De Smet, A.M.G.A., Diederen, B.M.W., Kluytmans, J.A.J.W., Van Keulen, P.H.J., 2007. Antimicrobial Agents and Chemotherapy 51 (10), 3726–3730.
Lorian, V., 1986. Antibiotics in Laboratory Medicine. Williams & Wilkins, Philadelphia.
Lutz, R., Bujard, H., 1997. Nucleic Acids Research 25 (6), 1203–1210.
Mancini, N., Carletti, S., Ghidoli, N., Cichero, P., Burioni, R., Clementi, M., 2010. Clinical Microbiology Reviews 23 (1), 235–251.
Martindale, W., 1989. Martindale: The Extra Pharmacopoeia. Pharmaceutical Press, London.
Mohan, R., Schudel, B.R., Desai, A.V., Yearsley, J.D., Apblett, C.A., Kenis, P.J.A., 2011. Sensors and Actuators B Chemical 160 (1), 1216–1223.
Mouton, J.W., 1999. Infection 27 (SUPPL. 2), S24–S28.
Nakamura, N., Shigematsu, A., Matsunaga, T., 1991. Biosensors and Bioelectronics 6 (7), 575–580.
Nicodemo, A.C., Araujo, M.R.E., Ruiz, A.S., Gales, A.C., 2004. Journal of Antimicrobial Chemotherapy 53 (4), 604–608.
Rasband, W., 2011. Image J.
Rice, L.B., 2010. Infection Control and Hospital Epidemiology 31 (SUPPL. 1), S7–S10.
Rolinson, G.N., 1980. Journal of General Microbiology 120 (2), 317–323.
Schudel, B.R., Choi, C.J., Cunningham, B.T., Kenis, P.J.A., 2009. Lab on a Chip 9 (12), 1676–1680.
Schudel, B.R., Tanyeri, M., Mukherjee, A., Schroeder, C.M., Kenis, P.J.A., 2011. Lab on a Chip 11 (11), 1916–1923.
Sia, S.K., Whitesides, G.M., 2003. Electrophoresis 24 (21), 3563–3576.
Sun, P., Liu, Y., Sha, J., Zhang, Z., Tu, Q., Chen, P., Wang, J., 2011. Biosensors and Bioelectronics 26 (5), 1993–1999.
Sung, J., Shuler, M., 2012. Annals of Biomedical Engineering 40 (6), 1289–1300.
Tan, T.Y., Ng, S.Y., 2007. Clinical Microbiology and Infection 13 (5), 541–544.
Theberge, A.B., Courtois, F., Schaerli, Y., Fischlechner, M., Abell, C., Hollfelder, F., Huck, W.T.S., 2010. Angewandte Chemie - International Edition 49 (34), 5846–5868.
Thorson, M.R., Goyal, S., Gong, Y., Zhang, G.G.Z., Kenis, P.J.A., 2011. CrystEngComm. 14 (7), 2404–2412.
Tipper, D.J., 1985. Pharmacology and Therapeutics 27 (1), 1–35.
Traub, W.H., 1970. Applied Microbiology 20 (1), 98–102.
Tsou, P.-H., Sreenivasappa, H., Hong, S., Yasuike, M., Miyamoto, H., Nakano, K., Misawa, T., Kameoka, J., 2010. Biosensors and Bioelectronics 26 (1), 289–294.
Udekwu, K.I., Parrish, N., Ankomah, P., Baquero, F., Levin, B.R., 2009. Journal of Antimicrobial Chemotherapy 63 (4), 745–757.
White, R.L., Burgess, D.S., Manduru, M., Bosso, J.A., 1996. Antimicrobial Agents and Chemotherapy 40 (8), 1914–1918.
Winslow, D.L., Damme, J., Dieckman, E., 1983. Antimicrobial Agents and Chemotherapy 23 (4), 555–558.
Xia, Y., Whitesides, G.M., 1998. Annual Review of Materials Science 28 (1), 153–184.